

Infrared properties of exotic superconductors.

T. Timusk

Department of Physics and Astronomy, McMaster University, Hamilton, Ontario, Canada L8S 4M1
(October 25, 2018, submitted to Heraklion Conference of unconventional superconductors.)

The infrared spectra of the non-traditional superconductors share certain common features. The lack of a gap signature at 2Δ and the residual conductivity are the consequence of a d-wave order parameter. The high T_c materials, the organic conductors and the heavy Fermion materials have a strong mid-infrared absorption band which can be interpreted as strong coupling of the carriers to electronic degrees of freedom which leads to a breakdown of the Fermi liquid picture. The cuprates and the organic charge transfer salts are unique in possessing an intrinsic low dimensionality. The charge transport normal to the highly conducting direction is incoherent down to the lowest temperatures and frequencies.

A. INTRODUCTION

The discovery of high temperature superconductivity (HTSC) by Bednorz and Müller [1] raised the question of the relationship between these materials and other, previously known unconventional superconductors such as the organic conductors, the bismuthates and the heavy Fermion materials. Since 1987 other novel superconductors such as the borocarbides [2] and the alkali fullerenes [3] have been discovered. The aim of this review is to examine, from the point of view of one experimental technique, infrared spectroscopy, several of these families of unconventional superconductors.

Optical spectroscopy has several advantages over other techniques for the analysis of the transport properties of a broad range of conducting systems. First, it is not surface sensitive since electromagnetic radiation penetrates a hundreds of nanometers into the crystal. Second, relatively small lateral sample dimensions of the order of $500\ \mu\text{m}$ are enough to yield high quality spectra in the interesting $200 - 1000\ \text{cm}^{-1}$ frequency region, a region relevant to the excitations in most superconductors. In contrast, more powerful techniques such as angle resolved photoemission or vacuum tunneling demand ultrahigh-vacuum cleaved, virgin surfaces and as a result have been applied to only a few systems. Magnetic neutron scattering, another powerful technique, due to the weak interaction of the neutron with matter, demands large centimeter size crystals which are simply not available for most new materials. As a result, optical spectroscopy has become the spectroscopic technique of choice for the investigation of the low lying excitations of a large range of new materials and doping levels.

Reflectance spectroscopy, combined with Kramers Kronig analysis, yields the real and imaginary parts of the optical conductivity. In systems with s-wave, dirty limit superconductivity, optical methods were first used to study the energy gap [4] and later the spectrum of excitations. [5–7]. It can also be used to determine the superconducting penetration depth tensor. And unlike the dc conductivity which becomes infinite in the superconducting state and shorts out all parallel channels of

conductivity, infrared techniques can be used to measure the optical conductivity of quasiparticles below T_c . [11] Even better results are obtained with the closely related technique, microwave absorption. [9]

In what follows we review the optical properties in the infrared of a range of unconventional superconductors as revealed by reflectance spectroscopy. We start by setting the stage with the discussion of conventional BCS superconductors and then move to several families of less and less conventional superconductors starting with materials that seem to be almost conventional but show clear signatures of deviation from familiar behaviour.

There is a grey area in all classification schemes. For unconventional superconductors it includes materials that are distinguished by high transition temperatures and where relatively little reliable infrared data exists. This includes materials such as the A15 compounds, [10] the borocarbides, and the doped fullerenes. Some of these materials are discussed by other contributors to this conference.

B. BCS SUPERCONDUCTORS IN THE INFRARED

One of the pioneering experiments in conventional superconductors was the measurement of the energy gap by far infrared reflectance spectroscopy by Tinkham and his collaborators [4]. The gap in the excitation spectrum of magnitude 2Δ leads to a region of unit reflectance for $h\nu < 2\Delta$. Above the gap frequency absorption sets in and the reflectance drops to the normal state value. Reflectance experiments in conventional metals are difficult since, in a good metal, the normal state absorption is very weak, typically $1 - R = 0.005$. To overcome the weak absorption, sensitive calorimetric techniques [5] or multiple reflection cavities [10] are used. The disadvantage of these methods is the difficulty of getting an absolute calibration.

The second important early contribution of infrared spectroscopy was the discovery of Joyce and Richards of phonon structure resulting from strong coupling effects,

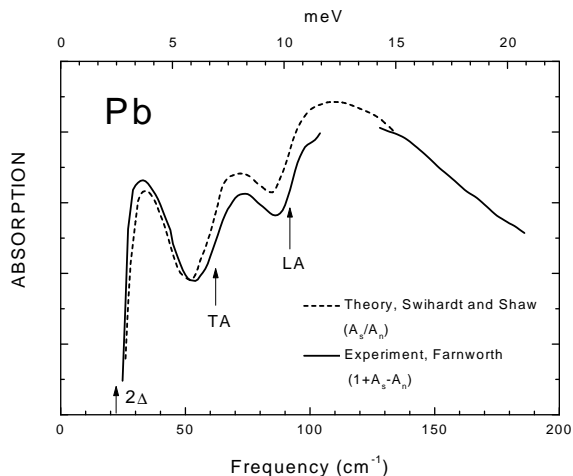


FIG. 1. Infrared absorption of lead in the superconducting state divided by the normal state absorption (arbitrary units). This conventional BCS superconductor does not absorb energy below 2Δ the superconducting gap and there is a sharp threshold of absorption at this frequency. There is a further increase in absorption at $h\nu = 2\Delta + \Omega_{TA}$ the onset of transverse acoustic phonon scattering and another one at the longitudinal frequency. The dashed curve is a theoretical one based on Eliashberg theory. There is excellent agreement between the theory and the experiment.

similar to the structure seen in tunnelling spectra. [5] Fig 1. shows, from the work of Farnworth, [10] the difference in the absorption of a lead film between the superconducting and normal states. A magnetic field was used to destroy the superconductivity. The rise in absorption at 22 cm^{-1} is due to the onset of normal state absorption at the gap energy at $h\nu = 2\Delta$. The double-peak structure above the gap energy is due the interaction of the superconducting carriers with transverse and longitudinal acoustic phonons. The dashed curve is a theoretical calculation by Swihart and Shaw [12] of the absorption ratio using a full Eliashberg theory including vertex corrections. The phonon spectrum of lead as determined by neutron scattering was used. It is clear from these data that it is possible to identify all the important features of a BCS superconductor with infrared reflectance spectroscopy: an infrared signature of BCS superconductivity is a region of unit reflectance that occurs below T_c followed by phonon structure that reflects the electron phonon density of states which is directly responsible for superconducting pairing.

As we will see in what follows, the unconventional superconductors do not show this simple behavior, but even in BCS superconductors there are many complications that go beyond the simple strong coupling behavior shown in Fig 1. For example, it is not always possible to see a gap signature and a phonon spectrum in the same sample. The onset of absorption at the gap frequency is due to the presence of impurities that allow for momen-

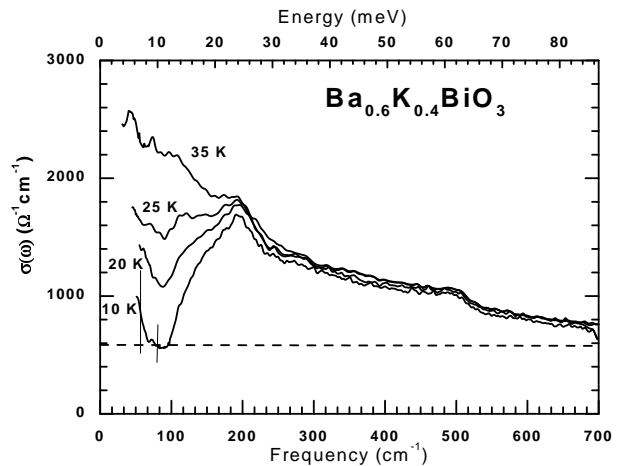


FIG. 2. The optical conductivity of BKBO at several temperatures. In the normal state (top curve) the conductivity has a Drude peak which has a temperature independent width, suggesting that the scattering is elastic due to impurities. As the temperature is lowered below the superconducting transition temperature a gap like depression develops in the conductivity. We associate this with an s-wave superconducting gap. There is no evidence of the phonon structure in the conductivity expected for conventional electron-phonon interaction.

tum conservation. In a clean superconductor absorption does not start at 2Δ but at frequencies where inelastic processes such as phonons can take up the momentum of the photon. Lead films such as those shown in Fig. 1 have some impurities that allow for a gap to be seen but not enough to dominate the scattering processes and suppress the electron phonon scattering. [13] A gap signature and phonons appear together in 3D metals where surface scattering processes result in apparent dirty limit behavior in pure crystals.

Furthermore, in pure 3D metals, there are surface scattering processes that result in apparent dirty limit behavior and allow a gap signature and phonons to appear in the same sample as shown in Fig. 1.

C. BKBO AN UNCONVENTIONAL OXIDE SUPERCONDUCTOR.

$\text{Ba}_{1-x}\text{K}_x\text{BiO}_3$ (BKBO), along with its cousin $\text{BaPb}_x\text{Bi}_{1-x}\text{O}_3$, form a family of superconductors with cubic perovskite structure in the superconducting phase where $x \approx 0.3$. [14] The transition temperature of BKBO is quite high (31 K) in relation to its low density of states at the Fermi level, and it has been suggested [15] that the material is closely related to cuprate high T_c superconductors. However the optical properties suggest that they are in fact closer to the conventional BCS superconductors than to the exotic cuprates.

Fig. 2 shows the optical conductivity at low frequency, at four temperatures, for $\text{Ba}_{0.6}\text{K}_{0.4}\text{BiO}_3$ with $T_c = 31$ K from the work of Puchkov *et al.* [16] Apart from a temperature independent background, indicated by a dashed line, the temperature behavior is that of a conventional BCS, slightly dirty, superconductor. The normal state is well fit by a Drude peak with a width of ≈ 230 cm^{-1} plus some direct transverse optical phonon absorption lines at about 200 and 500 cm^{-1} . A gap-like depression develops precisely at T_c and a gap *opens* as the temperature is reduced. The superconducting gap is $2\Delta = 90 \pm 10$ cm^{-1} and as T_c is varied with doping, the gap to T_c ratio is constant at $2\Delta/k_B T_c = 4.2 \pm 0.3$. This simple behavior should be contrasted with what is seen in the cuprates: there the gap develops already in the *normal state* (except in the limit of large overdoping), there is no 2Δ gap signature and the gap ratio is not constant—in the underdoped range the gap *decreases* as T_c is increased with doping. [17]

In BKBO, at 10 K, the conductivity below the gap frequency drops to a background conductivity shown as a dashed line. This background absorption level has been obtained by extrapolation from high frequencies. Puchkov *et al.* interpret the data in terms of two channels of conductivity, a Drude channel that undergoes a conventional superconducting transition and a second, possibly polaronic, channel that remains non-superconducting and is responsible for the broad temperature independent background. The two channel picture has also been advanced to explain the temperature dependence of the dc resistivity. [18] Thus the infrared conductivity of BKBO is that of dirty s-wave superconductor, a behavior that is quite different from what is seen in a dirty d-wave superconductor as we will see below.

Despite the development of a conventional gap structure below T_c , the BKBO spectrum does not show all the signatures of a conventional BCS phonon coupled superconductor, which in view of the large transition temperature is expected to be a strong coupling system. A detailed calculation, based on Eliashberg theory with phonons by Marsiglio *et al.*, bears this out yielding electron-phonons coupling $\lambda = 1$ and a transition temperature of 31 K. [19] As Fig. 3 shows, the imaginary part of the optical conductivity cannot be fit with this large value of λ but is fit well with $\lambda = 0.2$, a number that is clearly inconsistent with the large transition temperature and the assumed phonon spectrum taken from tunneling. [20] Sharif *et al.* have found a similar low value of λ based on tunneling measurements. They also conclude that BKBO is not an electron-phonon superconductor. [21] This weak coupling to phonons is consistent with the absence of Holstein phonon structure below T_c and as Fig. 2 shows there is no evidence of such structure in BKBO.

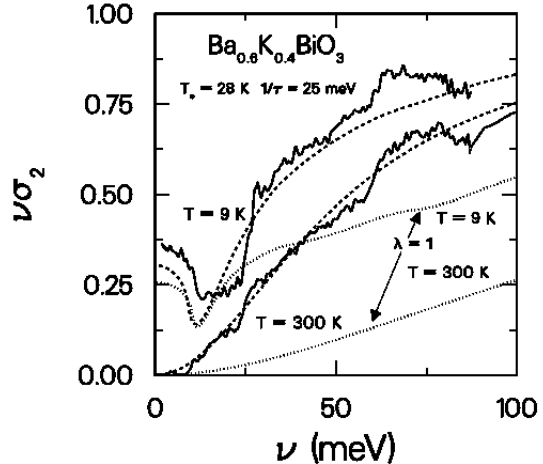


FIG. 3. The real part of the conductivity of BKBO (solid curves) and a theoretical calculation of the same quantity using Eliashberg theory with the electron-phonon interaction. There is a discrepancy between the coupling constant $\lambda = 0.2$ (dashes) needed to fit the infrared experiments, and $\lambda = 1$ needed to fit the high transition temperature.

D. Sr_2RuO_4 and URu_2Si_2 TWO FERMI LIQUID SUPERCONDUCTORS

In this section we discuss two materials that, at first sight appear unrelated, URu_2Si_2 a typical intermetallic compound showing heavy Fermion behavior at low temperature and Sr_2RuO_4 an oxide of Ru that is isostructural with the high T_c superconductor $\text{La}_{2-x}\text{Sr}_x\text{CuO}_4$ with the ruthenium replacing copper. However, a closer examination shows a surprising number of common elements of the two ruthenium containing materials. Both materials are superconductors with a rather low T_c of the order of 1 K. Infrared spectroscopy has not been used to investigate the gap structure in these two materials since the gap is expected to occur in the difficult submillimeter region and the normal state absorption will be very weak at these frequencies at low temperature. However, infrared can be used to study the normal state transport properties.

While the inplane resistivity of Sr_2RuO_4 is metallic, normal to the planes the resistivity (in the *c*-direction) shows a "semiconducting" temperature dependence above 130 K and a metallic one at low temperatures [22]. Similar behavior is seen in the resistivity of URu_2Si_2 in all directions with a maximum at 80 K [23]. Both materials become good conductors at low temperature with a T^2 dependence of the resistivity expected for a pure metal when the phonon scattering is frozen out. Superconductivity sets in at about 1 K.

The two ruthenium materials are very different in their electronic properties: URu_2Si_2 gets its poor metallic behaviour from strong incoherent scattering which freezes

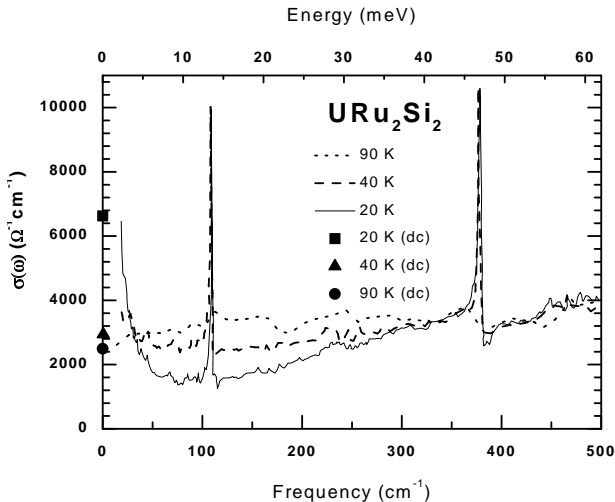


FIG. 4. The normal state conductivity of URu_2Si_2 . At high temperature the conductivity is flat and featureless due to the strong magnetic scattering. As the temperature is lowered below the coherence temperature T_K a coherent Drude peak develops at low frequency.

out for $k_B T < k_B T_K$ where $k_B T_K$ is a Kondo energy scale characteristic of magnetic scattering. Sr_2RuO_4 on the other hand is very anisotropic in its crystal structure with weak coupling between the current carrying RuO_2 planes. However at low temperature where $k_B T < t_\perp$ the planes couple coherently and the material becomes a very anisotropic 3D conductor.

In agreement with these ideas both systems develop sharp Drude peaks at low temperature which are signatures of good metals. Fig. 4 shows the optical conductivity of URu_2Si_2 . [24] At 90 K, well above the coherence temperature T_K the conductivity is flat and frequency independent. As the temperature is lowered, a Drude peak develops at low frequency, borrowing spectral weight from a frequency band that is a few times $k_B T_K$. As the temperature is lowered further, the peak sharpens. A detailed analysis of the spectrum in terms of a frequency dependent mass formalism shows that the carriers are massive with $m = 50m_e$ consistent with specific heat data in this heavy Fermion system.

A similar onset of coherence is seen in the c -axis conductivity of the quasi two-dimensional material Sr_2RuO_4 . Fig. 5 shows data of Katsufuji *et al.* of the c -axis conductivity. [25] The conductivity, apart from a few strong transverse phonon peaks, consists of a flat band with a slight Drude-like peak below 0.02 eV (160 cm^{-1}). Spectral weight is lost in the 100 to 200 cm^{-1} region to a narrowing Drude peak. The author's data does not extend low enough in frequency to resolve the peak but the dashed lines, fit to the increasing dc conductivity with decreasing temperature, show the expected conductivity. As in the case of URu_2Si_2 the area under the Drude peak is a small fraction of the total infrared spectral weight suggesting a large mass for c -axis motion. This is veri-

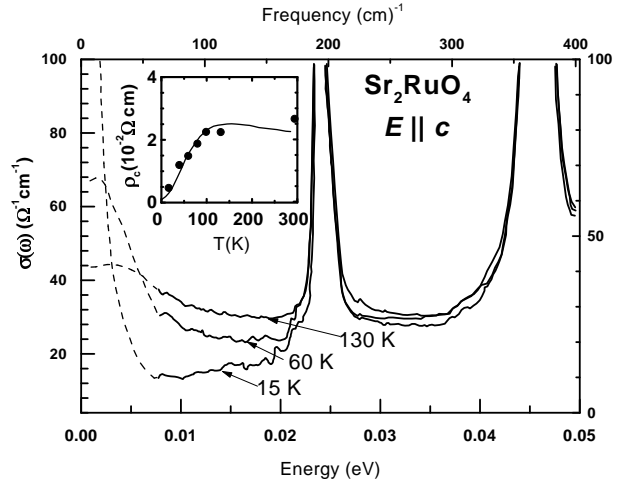


FIG. 5. The normal state conductivity of Sr_2RuO_4 . As in URu_2Si_2 , at high temperature the conductivity is flat, apart from direct LO phonon lines. Below 100 K , a temperature where thermal fluctuation energy is less than the coupling energy between the planes, a coherent Drude peak develops at low frequency.

fied by magneto oscillation experiments [26].

The two ruthenium containing systems behave in a very conventional way at low temperature, in that they are 3-D Fermi liquids, but at high temperature one shows effects of magnetism and the other of highly anisotropic transport properties. As we will see in the next two sections, combining both ingredients results in truly exotic behavior of the cuprates and the organic conductors.

E. THE CUPRATES

While the high superconducting transition temperature is the defining property of the HTSC cuprates, several properties set the cuprate family apart from the conventional BCS superconductors. These include the anomalous normal state resistivity as emphasized early by Anderson, [27] the d -wave superconducting order parameter, the magnetism, the two-dimensional transport, and finally the presence of a normal state pseudogap.

There is an extensive literature on the optical conductivity of the cuprates which has been reviewed recently by Basov and Timusk. [28] Here we focus on those features of the optical conductivity that make the cuprates unique: the lack of the 2Δ gap signature in the optical conductivity, the crucial role played by the two-dimensional nature of the transport and finally the the normal state pseudogap.

The absorption and the optical conductivity of a typical HTSC cuprate, $\text{YBa}_2\text{Cu}_3\text{O}_{7-\delta}$, is shown in Fig. 6. The normal state shows a Drude-like peak. Below T_c the spectral weight of the peak is transferred to the condensate delta function at $\omega = 0$ but there is no signature of

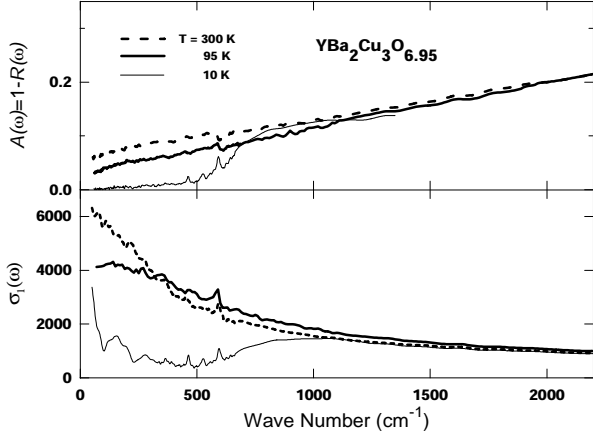


FIG. 6. The absorption $A = 1 - R$ and the optical conductivity for optimally doped Y123 with $x = 6.95$. A depression of A is seen below 800 cm^{-1} below the superconducting transition temperature T_c . There is a corresponding depression of conductivity in the superconducting state but because the system is in the clean limit with $1/\tau < 2\Delta$, the onset of conductivity and absorption is not the superconducting gap which can only be seen in the dirty limit.

a superconducting gap as seen in BKBO. Instead, there remains a weak continuous conductivity at all frequencies including in the region where one expects to see the superconducting gap. Careful study of the optical conductivity by various techniques shows that the width of the Drude peak diminishes by several orders of magnitude just below T_c [29,11,9,30] which suggests that a gap is formed in the spectrum of excitations responsible for the scattering of the carriers. This behaviour is in striking contrast to electron-phonon superconductors where there are no major changes to the phonon spectrum at the superconducting transition. In the cuprates the excitations are electronic and as a gap develops in these excitations a dramatic decrease in scattering takes place. The optical properties of the cuprates are those of a clean limit superconductor where the 2Δ transitions are forbidden because of momentum conservation. In this respect the cuprates behave exactly the same as the BCS superconductors. An obvious experiment to try would be to introduce impurities to approach the dirty limit.

Fig 7 shows the effect of defects on the optical conductivity of radiation damaged $\text{YBa}_2\text{Cu}_3\text{O}_{7-\delta}$ from the work of Basov *et al.* [31] As the defect concentration rises, a Drude-like peak, displaced slightly from zero frequency, grows. There is no sign of a peak at 2Δ , expected to be in the neighborhood of 600 cm^{-1} . This behavior is seen

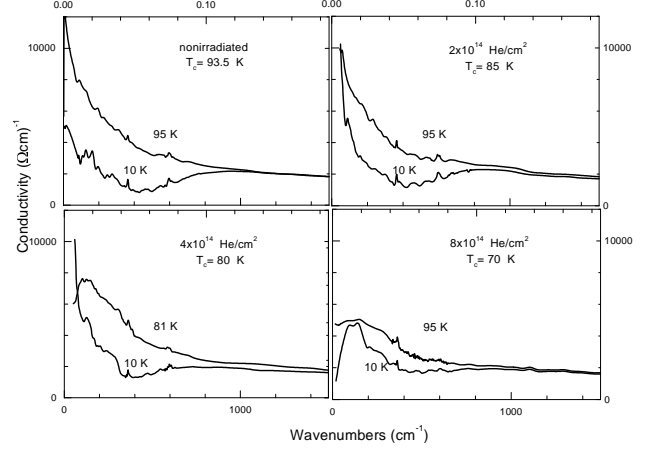


FIG. 7. The effect of impurities on a d-wave superconductor. Increased defect concentration does not yield a gap signature in the conductivity as seen in BCS superconductors. As the damage level is increased a Drude-like peak develops at low frequency. At high damage levels the peak moves to finite frequency.

in a number of cuprate systems containing either doped impurities [32] or other forms of disorder such as partial occupancy at oxygen sites [33,34] or radiation damage. [31] Recent work of Basov *et al.* shows similar effects in Zn doped $\text{YBa}_2\text{Cu}_3\text{O}_{7-\delta}$: there is no 2Δ gap signature and, in the superconducting state there is a Drude-like conductivity peak, shifted slightly from zero to finite frequencies. [32] A BCS s-wave superconductor is relatively insensitive to disorder where the main result of strong impurity scattering is the erasure of any gap anisotropy and the removal of the clean limit restriction on momentum conservation resulting in the familiar 2Δ gap signature. In contrast, in a d-wave superconductor impurity scattering has the effect of restoring part of the Fermi surface near the nodes and the optical conductivity acquires a low frequency component, very similar to a Drude peak. [35]

The second fundamental property of the cuprates is an intrinsic anisotropy of electronic transport that goes beyond the simple anisotropic effective mass seen for example in doped semiconductors or in the Sr_2RuO_4 system discussed above. Here we have a qualitative difference in the properties along the planes where the conductivity is coherent and metallic and perpendicular to the planes, in the c -direction, where the conductivity is incoherent down to the lowest temperatures and frequencies. Fig 8 shows the c -axis conductivity of a $\text{YBa}_2\text{Cu}_3\text{O}_{7-\delta}$ crystal that is slightly underdoped. Like the Sr_2RuO_4 discussed in the last section, at high temperature there is a broad, essentially frequency independent, absorption band and no coherent Drude peak. Since the material shown is underdoped it shows a depressed conductivity below 300 cm^{-1} due to the normal state pseudogap at low temper-

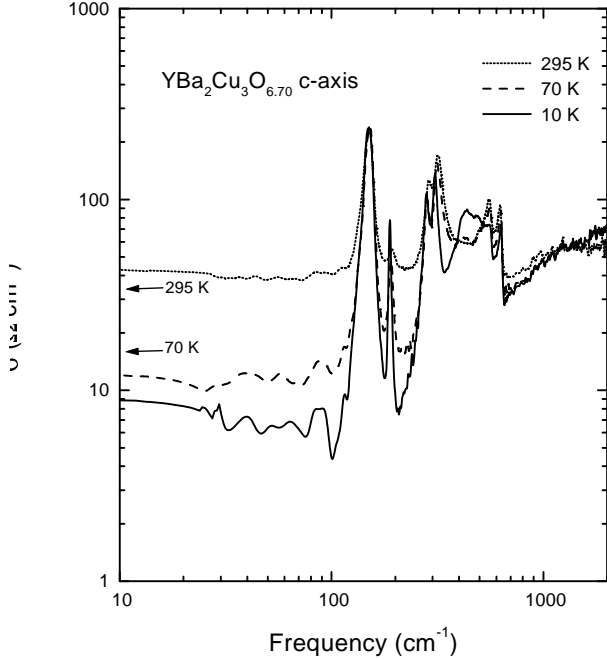


FIG. 8. Conductivity normal to the copper oxygen planes of $\text{YBa}_2\text{Cu}_3\text{O}_{7-\delta}$. Over two orders of magnitude in frequency, the electronic background conductivity is frequency independent. The peaks are due to optic phonons and the depression in conductivity below 300 cm^{-1} is due to the pseudogap.

ature [41] that will be discussed below. But down to the lowest frequency and temperature, there is no evidence of a Drude peak. The arrows denote the values of the dc resistivity and it clear that, at least above 70 K, there is no coherent conduction in this system. It is not possible to measure the dc resistivity below this temperature since the material becomes superconducting. Recent microwave measurements [42] show that the conductivity remains incoherent down to 22 GHz and 1.2 K.

Recent work using a variety of experimental probes, most strikingly angle resolved photoemission, [36,37] shows that the normal state of the high temperature superconductors is dominated by a partial gap, or a pseudogap. The experimental evidence has been reviewed recently by Timusk and Statt. [38] The pseudogap forms at a temperature T^* which is substantially above the superconducting transition temperature in most underdoped samples. T^* approaches T_c in YBCO near optimal doping. Just as infrared spectroscopy can show the collapse of scattering associated with the development of superconductivity, it also shows the loss of electron-electron scattering on formation of the pseudogap. As shown first

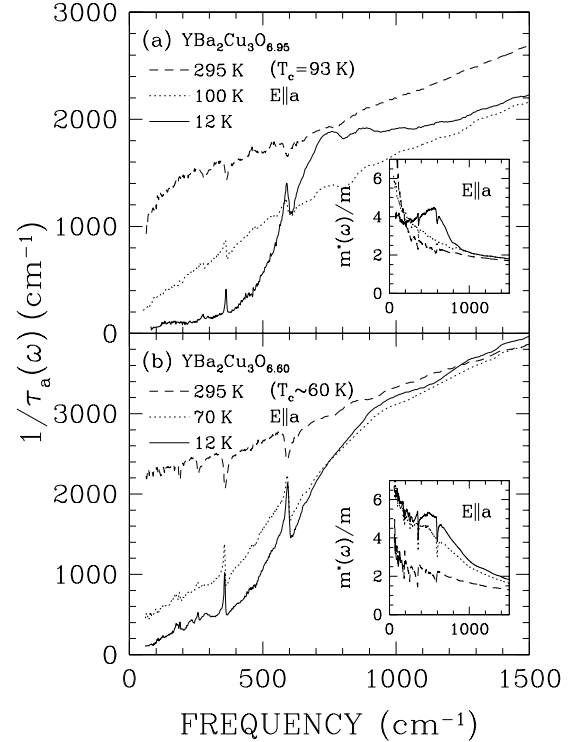


FIG. 9. Frequency dependent scattering rate of the holes in YBCO, a) optimally doped sample and b) an underdoped sample. In the optimally doped sample the scattering rate is linear in both frequency and temperature above T_c and develops a gap like depression below T_c . In the underdoped sample the scattering rate depression sets in well above T_c which is evidence of a normal state pseudogap. The insets show the effective mass of the carriers which show a characteristic resonance at 600 cm^{-1} .

by Basov *et al.* [39] and illustrated in Fig. 9, from a recent paper of Homes *et al.* [40] there is a loss of ab plane scattering associated with the formation of the pseudogap for frequencies below about 660 cm^{-1} .

Fig 8 shows a depression in the conductivity associated with the pseudogap that develops in this underdoped sample. There is a gaplike region of flat conductivity that fills in as the temperature is increased but there appears to be no change in the overall frequency scale of the conductivity as the temperature is raised – the gap fills in rather than closing. These measurements of the c-axis pseudogap by Homes *et al.* [41] were the first to yield spectroscopic evidence of the pseudogap. The c-axis pseudogap has since been observed in several other HTSC systems where samples of sufficient thickness are available [43,44] as well as in the ladder cuprates. [45]

In summary, infrared spectroscopy has revealed several exotic properties of the cuprates, the electronic coupling mechanism, possibly associated with magnetism, the in-

trinsic anisotropy and finally the presence of a pseudogap in the normal state. In what follows we will see that organic low-dimensional superconductors share some of these properties and that they are the properties that can be used to define exotic superconductivity.

F. THE ORGANIC SUPERCONDUCTORS

There are two main families of organic superconductors: conductors based on the two-dimensional (BEDT-TTF) organic molecule with a T_c in the neighborhood of 10 K, and the family of one-dimensional materials, the Bechgaard salts, based on the TMTSF molecule with a T_c just over 1 K.

There is surprisingly little known about the electronic properties of organic conductors largely because of the small size and fragility of the available crystals. Thus magnetic neutron scattering and angle resolved photoemission, powerful, momentum sensitive techniques, have not proven to be as useful here as they have been in the cuprates. While there is a considerable body of infrared spectroscopy, the strong mid-infrared absorption seen in the organics by all investigators is in clear contradiction with the extensive low temperature magnetic transport data. These contradictions in the interpretation of the experiments have lead to two completely opposing views of the normal state transport particularly in the Bechgaard materials where most of the work has been done.

Magnetic transport measurements have generally been interpreted in terms of Fermi liquid models with extraordinarily long scattering times. In agreement with this picture it is found that Kohler's rule holds [46] except for the conductivity component along the conducting chains. Various oscillatory phenomena have been seen in high fields and these have been interpreted in terms of electrons moving in quasi two-dimensional orbits. This interpretation of the data has been summarized by Greene and Chaikin [47]. Specific heat data [48] also suggest a superconducting transition from a normal metallic state.

The infrared community takes a diametrically opposed stand on the transport properties. Measurements of the frequency dependent conductivity at low temperature shows that the very large dc conductivity of $\approx 200,000$ $(\Omega\text{cm})^{-1}$ retains its large value well into the microwave region [49,50] but then drops dramatically in the 300 GHz range to a low value of ≈ 1000 $(\Omega\text{cm})^{-1}$. [54] The reflectance of such a system is expected to show a prominent plasma edge in the 300 GHz region, a difficult experimental region to work in with small needle like samples. Nevertheless, early far infrared work of Tanner's group as well as recent backward wave oscillator data from Grüner's group has shown evidence of this edge experimentally. [54,50] A clear observation of this edge confirms the picture of two component conductivity, a narrow Drude peak, presumably caused by a density

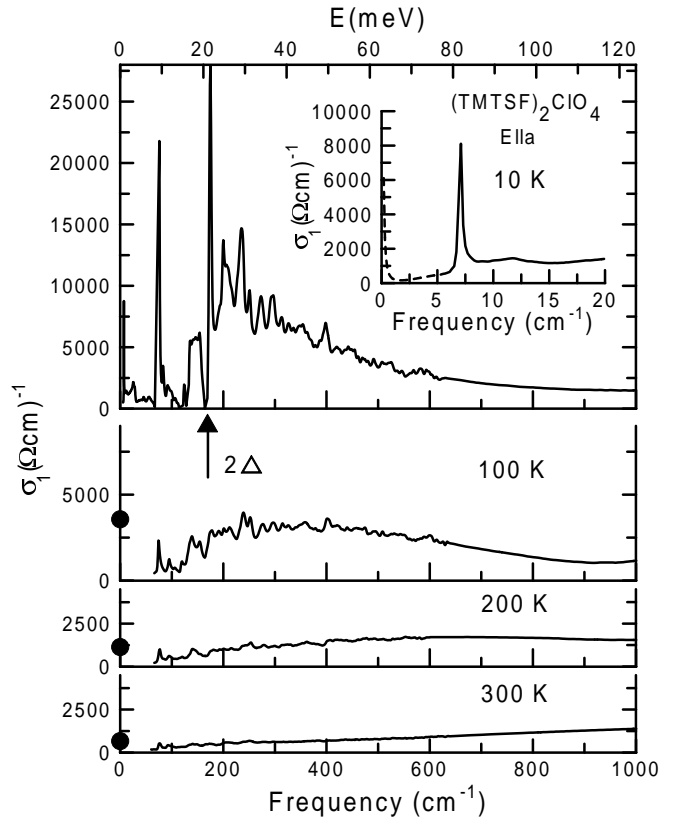


FIG. 10. Real part of $\sigma(\omega)$ of $(\text{TMTSF})_2\text{ClO}_4$ along the chain axis. The full circles on the left axis are the values of the dc conductivity. The 10 K dc value ($\sim 2 \times 10^5 \Omega^{-1}\text{cm}$) is too high to be shown on the scale used. A gap with the value $2\Delta \simeq 170 \text{ cm}^{-1}$ can be seen at 10 K. The inset is $\sigma(\omega)$ at 10 K between 5 and 20 cm^{-1} .

wave followed by a very broad incoherent band due to a strongly correlated Luttinger liquid.

Fig. 10 shows recent conductivity data of $(\text{TMTSF})_2\text{ClO}_4$ from Cao *et al.* for light polarized along the conducting chains. [52] We see, at room temperature, a broad incoherent band very similar to what is seen in the c -direction of the cuprates where the carriers are confined to the planes. The dc conductivity is not much larger than the infrared conductivity although there appears to be an incipient pseudogap already at room temperature.

As the temperature is lowered the dc conductivity increases and spectral weight is shifted to lower frequencies. A clear, gap-like depression, can be seen below 300 cm^{-1} . This behavior has also been seen in the charge density wave system TTF-TCNQ [53].

These data have been interpreted in terms of transport by charge density wave fluctuations. [54] Several characteristics point to this picture. First, there is a growth in the intensity of phonon lines as the temperature is lowered, behavior that is usually associated with sliding density waves interacting with the lattice. [55,56] Sec-

only, estimates of the spectral weight associated with the narrow low frequency mode of $\approx 500m_e$ suggest that phonons are involved as well. In this picture the peak in the far-infrared would correspond to direct transitions across the charge density wave gap [57].

The picture of transport along the chain axis by charge density wave fluctuations rests mainly on the assumption that strong infrared absorption is due to intrinsic bulk effects. It has been suggested that surface defects such as cracks may be responsible for the absorption and there is indeed scatter in the infrared data from various laboratories suggesting that sample quality may be a problem [52]. However it should be noted that the simple picture of cracks predicts that the absorption should continue well into the microwave range as long as the penetration depth is smaller than the crack depth.

There are several ways of investigating this problem. One of course is the use of samples with better controlled surfaces to see if the strong mid-infrared absorption is intrinsic. Assuming that it is, then reflectance measurements in high magnetic fields should be made to determine if sufficiently strong fields will break up the density waves and turn the materials into quasi one dimensional metals. There is preliminary evidence that this might be the case. [58]

Because of the low transition temperature and the low frequency range of the expected superconducting gap, little is known about the optical properties of the organic conductors in the superconducting state. It is hoped however, that when larger crystals become available, far infrared and microwave techniques will be used to investigate the issue of the superconducting gap as well as the transition region between the high dc and microwave conductivity and the strongly absorbing pseudogap range.

We finally touch briefly on the question of transport normal to the conducting chains. Fig 11 shows the infrared conductivity of $(\text{TMTSF})_2\text{ClO}_4$ in the b direction where there is considerable overlap between the chains (the third direction has even lower coupling between the chains). We again see a flat conductivity, similar to the case of the c-axis cuprates. There is some evidence of a collective mode since the dc conductivity is considerably higher than the infrared conductivity. However, the discrepancy is much smaller than what is observed in the chain direction. If one were to assign a scattering rate to this flat conductivity it would be of the order of 500 cm^{-1} (40 meV). This is to be compared with the estimated $t_{\perp} = 40$ meV, the transfer matrix element normal to the chains. In terms of a Fermi liquid picture, one would then expect that below a crossover temperature of $T = 40$ meV = 460 K coherence would develop and the material would become a 2D Fermi liquid. It is clear that down to 2 K there is completely incoherent transport between the chains.

In summary the organic superconductors display very anomalous properties in the infrared. There is no ev-

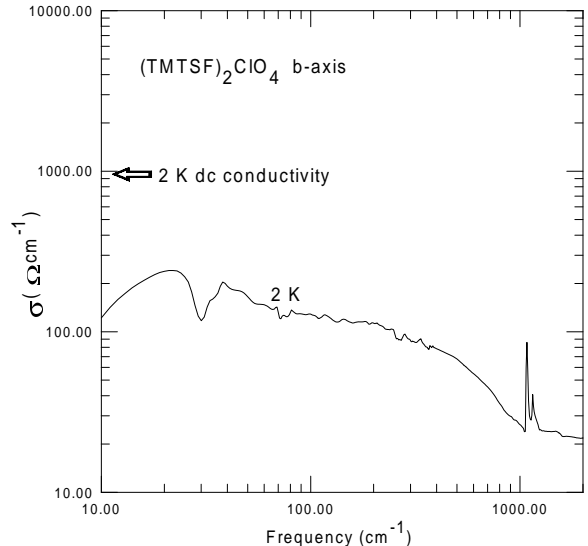


FIG. 11. Conductivity normal to the chain direction in $(\text{TMTSF})_2\text{ClO}_4$. The conductivity is flat and frequency independent. Its low value and lack of coherence suggests that the transport is incoherent normal to the conducting chains.

idence of simple metallic transport in any direction. Along the chains the currents are carried by collective modes, possibly sliding charge density waves while normal to the chains there is complete incoherence similar to what is seen in interplane transport in the cuprates.

G. CONCLUSIONS

We have discussed in this review an infrared view of the transport properties of a variety of superconductors, from the conventional BCS strong coupling superconductor lead, to the exotic cuprates and organic charge transfer materials. The focus has been on several markers of deviation from classic phonon-coupled systems: 1) the collapse of scattering at T_c , a signature of an electronic mechanism since phonon scattering is unaffected, to first order, by the formation of a gap in the electronic system, 2) the growth of a Drude peak in the superconducting state of dirty samples and absence of a 2Δ gap feature, both signatures of an order parameter with nodes 3) the role of intrinsic dimensionality that goes beyond simple anisotropy where we find that the carriers are confined to planes and chains and interplane/chain conductivity is incoherent down to the lowest temperatures and frequencies, 4) the presence of a pseudogap in the normal state associated with charge transport by complex objects.

For a true classification of all superconductors into anomalous and exotic varieties, as opposed to conventional ones, one needs data from all experimental techniques. Nevertheless the infrared is a good initial tool for this task since it can be applied to a wide range of ma-

terials being relatively modest in the demands it places on the crystal growers, who are of course responsible for much of the past progress in our understanding of unconventional superconductivity.

Acknowledgements.

I would first like to acknowledge Georgorgios Varelogiannis for the suggestion to undertake this survey of the infrared properties of unconventional superconductors and Jules Carbotte for valuable discussions on all aspects of superconductivity. The results described in this paper come in most part from the work of D.N. Basov, D.B. Bonn, N. Cao, B.F. Farnworth, C.C. Homes, H.K. Ng, R. Hughes, J.J. McGuire, A. Puchkov, M. Reedyk, T. R oom T. Strach and T. Startseva at McMaster. I thank Y. Tokura for permission to use Fig. 5. The crystal growers responsible for these results are K. Bechgaard, D. Colson, B. Dabrowski, S. Doyle, P. Fournier, J.D. Garrett, P.D. Han, A.M. Hermann, N. T. Kimura, K. Kishio, N.N. Kolesnikov, H.A. Mook, M. Okuya, R. Liang, W.D. Mosley and D.A. Payne. To them the experimentalists owe much.

-
- [1] J.G. Bednorz and K.A. M uller, *Zeitschrift f ur Physik* **64**, 189, (1986).
- [2] R.J. Cava *et al.* *Nature* (London) **367**, 252, (1994), Nagarajan *et al.* *Phys. Rev. Lett.* **72**, 274, (1994), B.K. Cho, P.C. Canfield, and D.C. Johnston, *Phys. Rev. B* **52**, R3844, (1995).
- [3] A.F. Hebard *et al.* *Nature* (London) **347**, 354, (1990).
- [4] R.E. Glover, III, and M. Tinkham, *Phys. Rev.* **108**, 243, (1957), D.M. Ginsberg and M. Tinkham, *Phys. Rev.* **118**, 990, (1960), P.L. Richards and M. Tinkham, *Phys. Rev.* **119**, 575, (1960).
- [5] R.R. Joyce and P.L. Richards, *Phys. Rev. Lett.* **24**, 1007, (1970).
- [6] B. Farnworth and T. Timusk, *Phys. Rev B* **10**, 2799, (1974).
- [7] B. Farnworth and T. Timusk, *Phys. Rev B* **14**, 5119, (1976).
- [8] D.B. Romero, C.D. Porter, D.B. Tanner, L. Forro, D. Mandrus, L. Mihaly, G.L. Carr, and G.P. Williams, *Phys. Rev. Lett.* **68**, 1590, (1992).
- [9] D.A. Bonn, P. Dosanjh, R. Liang, and W.N. Hardy, *Phys. Rev. Lett.* **68**, 2390, (1992).
- [10] B.F. Fanworth, Thesis, McMaster University (1995).
- [11] D.B. Romero, C.D. Porter, D.B. Tanner, L. Forro, D. Mandrus, L. Mihaly, G.L. Carr, and G.P. Williams, *Phys. Rev. Lett.* **68**, 1590, (1992).
- [12] J.C. Swihart and W. Shaw *Physica* **55**, 678, (1971).
- [13] P.B. Allen, *Phys. Rev B* **3**, 305, (1971).
- [14] L.F. Mattheiss E.M. Gyorgy, and S.E. Johnson, Jr., *Phys. Rev. B* **37**, 3745, (1988).
- [15] B. Batlogg, in *Mechanisms of High Temperature Superconductivity*, edited by H. Kamimure and A. Oshiyama, Springer Series in Materials Science (Springer, New York, 1989), Vol. 11, p. 342.
- [16] A.V. Puchkov, T. Timusk, W.D. Mosley and R.N. Shelton, *The Physical Review B* **50**, 4144-4153, (1994).
- [17] Ch. Renner, B. Revaz, J-Y Genoud, K. Kadowaki, and O. Fischer *Phys. Rev. Lett.* **80**, 149, (1998).
- [18] E.S. Hellman and E.H. Hartford, Jr. *Phys. Rev. B* **47**, 11346 (1993).
- [19] F. Marsiglio, J.P. Carbotte, A. Puchkov, and T. Timusk, *Phys. Rev B* **53**, 9433 (1996).
- [20] J.F. Zasadzinski, N. Tralshawala, Q. Huang, K.E. Gray, and D.G.Hinks, in *Electron phonon interaction in oxide superconductors* R. Baquero, editor, (World Scientific Singapore, 1991) p. 46.
- [21] F. Sharifi, A. Pargellis, R.C. Dynes, B. Miller, E.S. Hellman, J. Rosamilia, and E.H. Hartford, Jr., *Phys. Rev B* **44**, 12521, (1993).
- [22] Y. Maeno, H. Hishimoto, K. Yoshida, S. Nishizaki, T. Fujita, J.G. Bednorz, and F. Lichtenber, *Nature* **372**, 532 (1994).
- [23] T.T. Palstra, A.A. Menovsky, and J.A. Mydosh, *Phys. Rev. B* **33**, 6527 (1986).
- [24] D.A. Bonn, J.D. Garrett, and T. Timusk, *Phys. Rev. Lett.* **61**, 1305, (1988).
- [25] T. Katsufuji, M. Kasai, and Y. Tokura, *Phys. Rev. Lett.* **76**, 126 (1996).
- [26] A.P. Mackenzie, S.R. Julian, A.J. Diver, G.J. McMullan, M.P. Ray, G.G. Lonzarich, Y. Maeno, S. Nishizaki, and T. Fujita, *Phys. Rev. Lett.* **76**, 3786 (1996).
- [27] P.W. Anderson and Z. Zou, *Phys. Rev. Lett.* **60**, 132, (1988).
- [28] D.N. Basov, and T. Timusk, *Infrared Properties of High- T_c Superconductors: an Experimental Overview* in Handbook on the Physics and Chemistry of Rare Earths Edited by K.A. Dschneidner, LeRoy Eyring and M.B. Maple, North-Holland 1999.
- [29] M.C. Nuss, P.M. Mankiewich, M.L. O'Malley, E.H. Westervick, and P.B. Littlewood, *Phys. Rev. Lett.* **66**, 3305, (1991).
- [30] A. Hosseini, R. Harris, S. Kamal, P. Dosanjh, J. Preston R. Liang, W.N. Hardy, and D.A. Bonn, cond-mat/9811041
- [31] D.N. Basov, A.V. Puchkov, R.A. Hughes, T. Strach, J. Preston, T. Timusk, D.A. Bonn, R. Liang and W.N. Hardy, *Phys. Rev. B* **49**, 12165, (1994).
- [32] D.N. Basov, B. Dabrowski, and T. Timusk, *Phys. Rev. Letters* **81**, 2132, (1998).
- [33] J.S. Xue, M. Reedyk, J.E. Greedan, and T. Timusk *J. of Solid State Chem.* **102**, 492, (1993).
- [34] T. Timusk, D.N. Basov, C.C. Homes, A.V. Puchkov, and M. Reedyk *J. of Superconductivity* /bf 8, 437, (1994).
- [35] J.C. Carbotte, C. Jiang, D.N. Basov, and T. Timusk, *Phys. Rev. B* **51**, 11798, (1995).
- [36] A.G. Loeser, Z.-X. Shen, D. S. Dessau, D. S. Marshall, C. H. Park, P. Fournier, and A. Kapitulnik, *Science* **273**, 325, (1996).
- [37] H. Ding, T. Yokoya, J.C. Campuzono, T. Takahashi, M. Randeria, M.R. Norman, T. Mochiku, K. Kadowaki, T. Takeuchi, and J. Giapinzakis *Nature* **382**, 51, (1996).
- [38] T. Timusk and B. Statt, The pseudogap in high temperature superconductors: an experimental survey. Reports

- of Progress in Physics **62**, 61 (1999).
- [39] D.N. Basov, R. Liang, B. Dabrowski, D.A. Bonn, W.N. Hardy, and T. Timusk, Phys. Rev. Lett. **77**, 4090, (1996).
 - [40] C.C. Homes, D.A. Bonn, R.L. Liang, W.N. Hardy, D.N. Basov, T. Timusk, and B.P. Clayman (unpublished).
 - [41] C.C. Homes, T. Timusk, R. Liang, D.A. Bonn, and W.N. Hardy, Phys. Rev. Lett. **71**, 1645 (1993).
 - [42] A. Hosseini S. Kamal, R. Liang, D.A. Bonn, and W.N. Hardy, Phys. Rev. Lett. **81**,1298, (1998).
 - [43] D.N. Basov, H.A. Mook, B.Dabrowski, and T. Timusk Phys. Rev. B, **52**, R13141, (1995).
 - [44] M. Reedyk, T. Timusk, J.S. Xue and J.E. Greedan Phys. Rev B **56**, 9134, (1997).
 - [45] T. Osafune, N. Motoyama, H. Eisaki, and S. Uchida, unpublished
 - [46] L. Forró, K. Biliaković, and J.R. Cooper, Phys. Rev. B **29**, 2839, (1984).
 - [47] R.L. Greene and P.M. Chaikin, Physica B, **126** 431, (1984).
 - [48] P. Garoche, R. Brusetti, D. Jérôme, and K. Bechgaard J. Physique Lett. **43**, L147, (1982).
 - [49] B. P. Gorshunov, G. V. Kozlov, A. A. Volkov, V. Železný, J. Petzelt, and C. S. Jacobsen, Solid State Comm. **60**, 681, (1986).
 - [50] M. Dressel, A. Schwartz, G. Grüner, and L. Degiorgi, Phys. Rev. Lett. **77**, 398, (1996).
 - [51] D.B.Tanner, C.S. Jacobsen, A.F. Garito, and A.J. Heeger, Phys. Rev. Lett., **32** 1301, (1974).
 - [52] N. Cao, T. Timusk, and K. Bechgaard J. Phys. I France **6**, 1726, (1996).
 - [53] H. Basista, D.A. Bonn, T. Timusk, J. Voit, D. Jérôme, and K. Bechgaard, Phys. Rev. B **42**, 4088, (1990).
 - [54] D.B.Tanner, C.S. Jacobsen, A.F. Garito, and A.J. Heeger, Phys. Rev. Lett., **32**, 1301, (1974).
 - [55] M.J. Rice, Phys. Rev. Lett. **37**, 36, (1976).
 - [56] M.J. Rice, L. Pietronero and P. Bruesch, Solid State Comm. **21**, 757, (1977).
 - [57] P.A. Lee, T.M. Rice, and P.W. Anderson, Phys. Rev. Lett., **31**, 462, (1973); Solid State Comm., **14**, 703, (1974).
 - [58] H.K. Ng, T. Timusk, and K. Bechgaard, J. Phys. (Paris), Colloq. **3** C-867, (1983).